MDPI

Article

Fine Blanking of Austenitic Stainless Steel Gears Using Carbon-Supersaturated High-Speed Steel Tools

Tatsuhiko Aizawa [1,*] **and Kenji Fuchiwaki** [2]

1 Surface Engineering Design Laboratory, Shibaura Institute of Technology, 3-15-10 Minami-Rokugo, Ota, Tokyo 144-0045, Japan
2 Hatano Seimitsu, 183-7 Hirasawa, Hatano, Kanagawa 257-0015, Japan; kenji-fuchiwaki@hatanoseimitsu.co.jp
* Correspondence: taizawa@sic.shibaura-it.ac.jp; Tel.: +81-3-6424-8615

Abstract: Austenitic stainless steel gears were fabricated via the fine blanking process that can be used for mass production. A carbon-supersaturated (CS)-matrix high-speed steel punch was prepared to minimize the adhesive and abrasive wear damage. Its edge profile was tailored and finished to control the local metal flow around the punch edges and edge corners. This CS punch was utilized in fine blanking the AISI304 austenitic stainless steel gears. Ball-on-disc (BOD) testing was first employed to describe the frictional behavior of the CS tool steel disc against the AISI304 stainless steel balls. SEM-EDX analysis on the wear track revealed that a free-carbon tribofilm was formed in situ in the wear track to prevent adhesive wear via galling on the tool steel disc. No significant adhesive or abrasive wear was detected on the punch edges and punch edge corners after continuously fine blanking with 50 strokes. AISI304 gears were produced to have fully burnished surfaces. Their pitches, widths and circles were measured to evaluate their gear-grade balancing during the fine blanking process. The stabilized gear-grade balancing in JIS-9 to JIS-10 grades was attained for these as-blanked AISI304 gears without finishing processes.

Keywords: fine blanking; austenitic stainless steel gears; carbon supersaturation; high-speed steel punch; in situ solid lubrication; free-carbon tribofilm; gear-grade balancing

1. Introduction

Steel gears have been widely utilized as essential mechanical elements in reducers for machinery, robotics and automotive units [1]. Almost all the steel gears are tooth-cut in the traditional way with careful note of their geometric accuracy. Stainless steel gears are widely utilized in machinery due to their high strength–ductility balance and toughness [2]. In addition, small-scale stainless steel gears are selected for working in corrosive conditions, as reported in [3,4].

A fine blanking process has been used as an approach to fabricate small- and medium-sized steel gears [5]. It was attractive since it can yield fully burnished surfaces in mass production. Under severe shearing conditions, the abrasive wear of the blanking punch became an issue [6]. When fine blanking ductile materials such as austenitic stainless steels or titanium alloys, the fine-blanking punch often suffered from adhesive wear, where the fresh work fragments and their oxide debris particles adhered onto the punch surfaces [7]. The punch and die were easily damaged when fine blanking difficult-to-form work materials without pretreatment. In addition to this damage to the tools, the polishing and cleansing of those deposits on the die and punch surfaces significantly pushed up the production cost.

Low-dimensional materials such as MoS_2, graphite and h-BN have been recognized as a medium for superlubrication with an ultralow friction coefficient [8]. Among them, graphene or sp2-structured carbon is theoretically identified as a superlubricant [9]. In addition, many studies paid attention to the in situ solid lubrication mechanism of amorphous carbon films [10].

The carbon-supersaturation of punches and dies worked as a pretreatment to form a free-carbon tribofilm in situ on the contact interface of punch and die side surfaces with ductile work material during fine blanking processes [11]. The punch edge profile design was necessary to minimize the abrasive wear volume at the edges and corners, as stated in [12,13]. An industrial-grade titanium gear was fabricated without galling and with low abrasive wears at the punch edge. Austenitic stainless steel gears with higher dimensional accuracy were fabricated through increasing the forming steps in the fine blanking procedure in [14]. The fully burnished surface was difficult to attain thoroughly only advancing the fine blanking steps, even under a multi-step procedure.

In the present paper, carbon-supersaturation (CS) and punch edge profiling are utilized to prepare the gear-shaped punch for a continuous fine blanking process to yield AISI304-type austenitic stainless steel gears in a single step. The CS procedure via low-temperature plasma carburizing is explained together with the punch edge profiling and gear-grade balancing qualification. The ball-on-disc method is first employed to measure the friction coefficient of the CS tool steel disc against the AISI304 balls. A friction coefficient much lower than 0.15 with a sliding distance up to 500 m proves that the interface between the CS disc and AISI304 ball is lubricated in solid by the in situ-formed carbon tribofilm on the hot spots in the contact interface. Next, the CS-matrix high-speed steel-type YXR7 punch with a gear-shaped head and double chamfers is prepared for fine blanking experiments. The punch edge profile and AISI304 blanks are measured to describe the abrasive wear growth during fine blanking and to discuss the change in the gear-grade balancing with increasing number of strokes in the fine blanking process. No adhesive wear on the CS-YXR7 punch surfaces occurs even after continuously fine blanking the AISI304 plates up to 50 strokes. The abrasive wear width at the punch edges is significantly reduced to trace levels in less than 10 μm after 50 continuous strokes. High-grade balancing of fine-blanked gears is preserved in grades of JIS-9 to JIS-10 even without a finishing step.

2. Materials and Methods

A low-temperature plasma carburizing system was utilized to fabricate the CS-tool steel disc and the CS-matrix high-speed steel punch. This CS-punch was used for continuous fine blanking experiments. Radar classification was utilized to describe gear-grade balancing with an increasing number of strokes in the fine blanking process for the feasible evaluation of CS-punch edge profile control.

2.1. Carbon-Supersaturation Process

The plasma carburizing system, including the hollow cathode device, is schematically illustrated in Figure 1a. The punch was located lateral to the hollow cathode to intensify the carbon ion and CH-radical densities for carbon-supersaturation. RF (radio frequency) plasma was ignited using the dipole electrodes. DC (direct current) plasma was also induced, and the bias voltage was applied to the bottom plates of the hollow cathode. After preliminary parametric surveys on these processing parameters, the RF voltage and the DC bias were selected to be constant at +220 V and −400 V, respectively, in the following experiments. After evacuation down to the base pressure of 0.01 Pa, argon gas was introduced into a chamber (Figure 1b) at RT (room temperature) to perform plasma cleaning of the punch and die surfaces via argon ion bombardment. After increasing the process temperature up to 673 K under the argon atmosphere, the hydrogen gas was also mixed with the argon gas at a flow rate of 160 mL/min for argon and 20 mL/min for hydrogen. The total pressure was kept constant at 70 Pa. After presputtering with the DC plasma for 1.8 ks, methane gas was introduced as a carbon source into the argon and hydrogen mixture gas at a flow rate of 20 mL/min. At the specified duration of 14.4 ks, the specimen was cooled down in the chamber under a nitrogen atmosphere before evacuation down to atmospheric pressure. The processing temperature was monitored in situ using a thermocouple, which was embedded into the base plate below the hollow cathode device in Figure 1a. The total pressure and flow rates of the argon, hydrogen and methane gases were

also monitored for process control. As studied in [11–13,15], no iron or chromium carbides were synthesized in the plasma-carburized layer. The carbon-supersaturation process was characterized by a peak shift of α-ion in the tool steel to the lower 2θ angles in the XRD analysis. This detected peak shift was induced by the carbon solute occupation of the octahedral vacancy sites of α-ion lattices in the carburized layer. The carbon-supersaturated tool steel had a hardness higher than 1200 HV. The carbon-supersaturated layer at 673 K for 14.4 ks reached 40 μm in thickness.
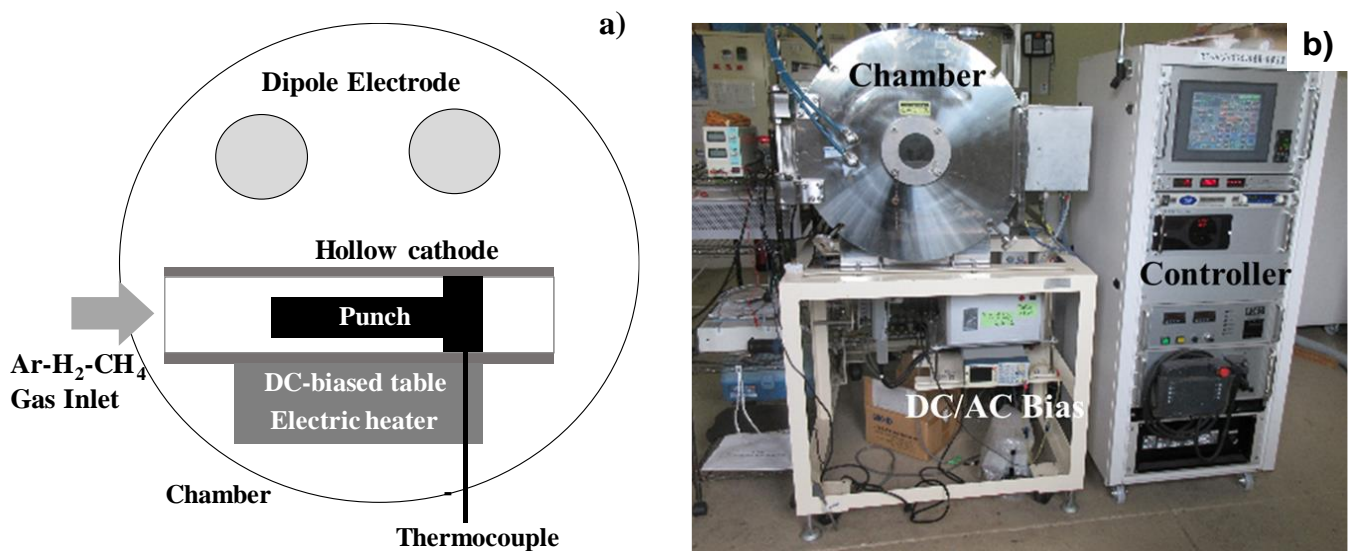
Figure 1. An experimental setup for low temperature plasma carburizing system. (**a**) Its schematic view and (**b**) its overview.

2.2. Fine Blanking System

- An austenitic stainless steel type AISI304 plate with a thickness of 2.0 mm, was fine-blanked with a narrow clearance of 0.5% as illustrated in Figure 2a. The hydraulic stamper (FB 160-FDE; Mori Iron Works Co., Ltd.; Saga, Japan), specially accommodated for the fine blanking process, was used for this experiment as shown in Figure 2b.
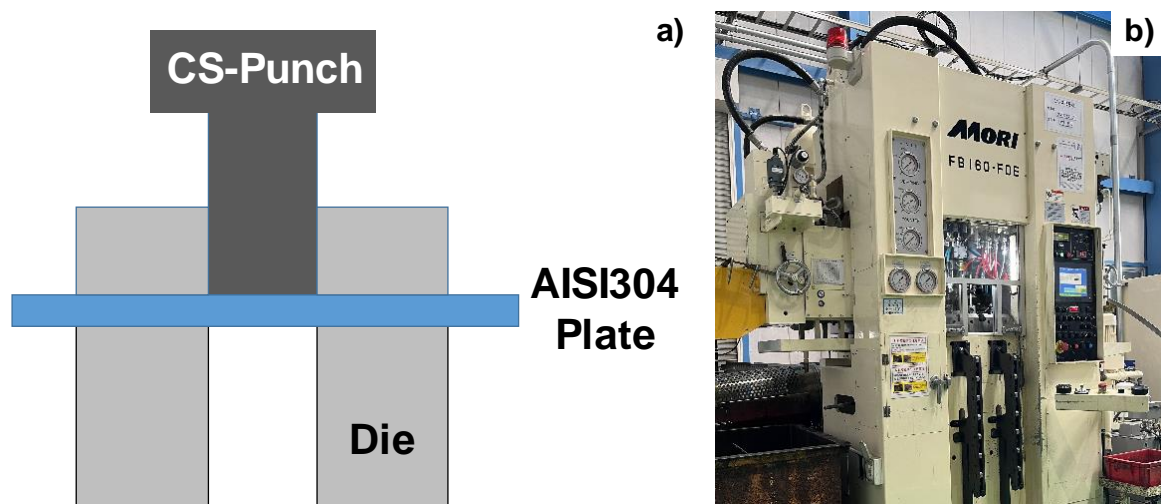
Figure 2. An experimental setup in the fine blanking at RT. (**a**) Its schematic view and (**b**) hydraulic stamping system for experiments.

The maximum loading capacity was 1600 kN. The loading sequence for fine blanking was CNC-programmed. These CS-punches were used to describe the effect of carbon supersaturation on the galling behavior. Each punch was fixed into the punch holder, which was further set up into the upper die set.

In the following experiments, FBH9-HMC with a viscosity of 101 m^2/s was utilized as a lubricating oil. A matrix high-speed steel type YXR7 punch with a controlled edge profile for the fine blanking of gears was depicted in Figure 3a. As explained in Figure 3b, each punch edge was finished to have a double chamfer for controlling the local metal flow in the vicinity of the edge corner. This finished YXR7 punch with double chamfered edges was plasma-carburized as a CS-YXR7 punch to be used in the following fine blanking experiments.
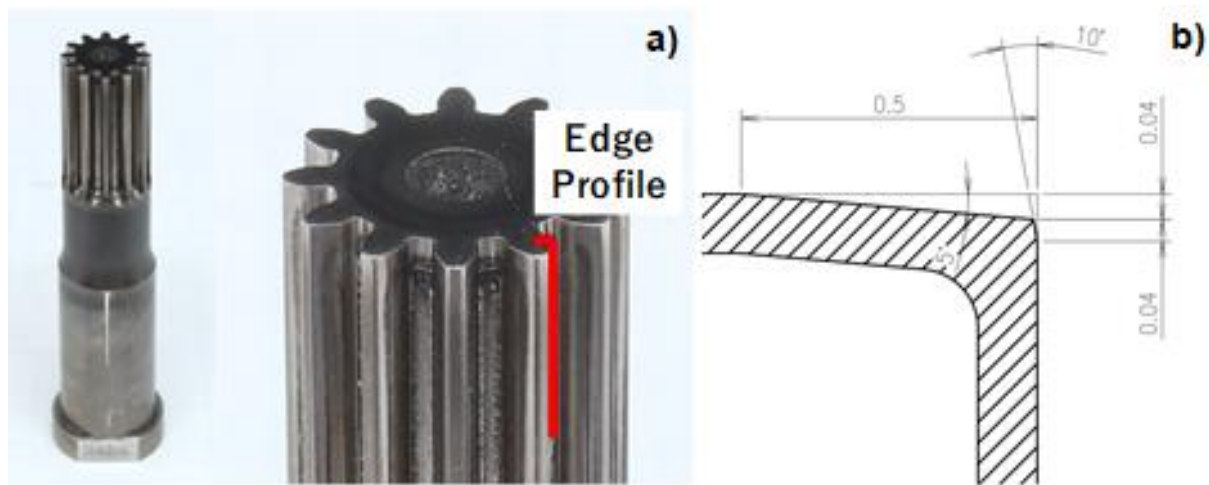

Figure 3. CS-YXR7 matrix high-speed steel punch with the tailored edge profile control for fine blanking the austenitic stainless steel gears. (**a**) Overview of the CS-YXR7 punch for fine blanking the gears and (**b**) tailored edge profile.

This matrix high-speed steel had a chemical composition as follows; carbon by 0.8 mass%, silicon by 0.8 mass%, manganese by 0.3 mass%, chromium by 4.7 mass%, tungsten by 1.3 mass%, molybdenum by 5.5 mass%, vanadium by 1.3 mass%, and iron in balance.

2.3. Radar Classification on the Blanked Gears

The radar classification method was employed to quantitatively describe the gear-grade balancing with increasing the strokes (N) during the fine blanking process. A three-dimensional profilometer with the aid of data-editing software was utilized to measure the tooth profile and alignment, the tooth pitch and the tooth space.

Figure 4 depicts the gear-grade balancing diagram in five dimensional deviations such as the total tooth profile deviation (F_α), the total tooth alignment deviation (F_β), the accumulated pitch deviation (F_p), the circular pitch individual deviation (f_p) and the tooth space run-out deviation (F_r). The smaller pentagonal diagram represents that the fine-blanked gear is fabricated with higher dimensional accuracy or with smaller JIS-grade after the Japan Industrial Standard [16]. The invariance of pentagonal size to N proves that no wear advances any more with increasing N during fine blanking.
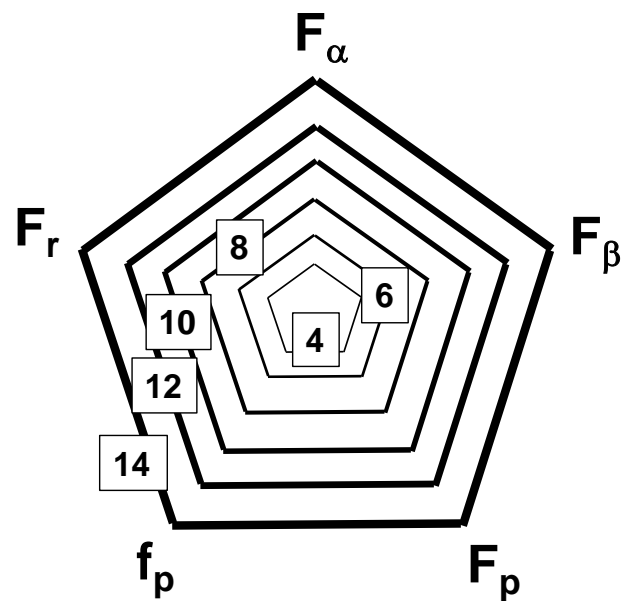
Figure 4. A gear-grade balancing diagram for evaluation on the dimensional accuracy of the fine blanked gears. Each number represents the JIS-grade; smaller number denotes for high dimensional accuracy on the gear tooth structure.

2.4. BOD Testing System

The ball-on-disc (BOD) testing system (Tribometer; CSM, Switzerland) was employed to describe the frictional behavior between the CS-SKD11 disc and the AISI304 austenitic stainless steel ball under the rotational sliding. This disc, with a diameter of 60 mm and a thickness of 5 mm, was plasma-carburized to prepare the CS-SKD11 disc in similar way to the carbon supersaturation of tool steel punches for fine blanking. The stainless steel AISI304 ball with a diameter of 6 mm was used as a counter material. The friction coefficient was defined, dividing the measured shear stress by the applied normal stress. In the following experiment, the applied load and sliding velocity were kept constant at 10 N and 100 mm/s, respectively.

2.5. Work Materials for Fine Blanking

The austenitic stainless steel type AISI304 plate with a thickness of 2 mm was employed as a work material for fine blanking in cold. Its chemical composition was listed as follows: e.g., 0.06 mass% carbon, 0.9 mass% silicon, 1.8 mass% manganese, 0.03 mass% phosphorus, 0.010 mass% sulfur, 8.5 mass% nickel, 18.5 mass% chromium, and iron in balance. Its surface roughness was equivalent to the as-rolled work.

3. Results

BOD testing is utilized to describe the friction behavior of the contact interface between the CS-SKD11 disc and the AISI304 ball. The CS-YXR7 punch, with its controlled edge profile, is prepared for continuously fine blanking the AISI304 plates up to 50 strokes. The contour measurement of punch edge profiles proves that adhesive wear or galling wear is significantly reduced. The gear-grade balancing measurement demonstrates that the high quality of the dimensional accuracy of AISI304 gears is preserved in their mass production without mechanical finishing.

3.1. BOD Testing

The variation in the measured friction coefficient with increasing sliding distance is depicted in Figure 5. Except for the initial running time, the friction coefficient was nearly held constant at 0.11 to 0.10 even under dry conditions without any lubrication. In the literature, the frictional behavior of tool steels against the stainless steels in sliding contact

was reported elsewhere [17,18]. The friction coefficient under dry conditions was higher than 1.0 even after sliding for 10 to 30 m under the applied load of 6N [18], while this high friction coefficient was suppressed down to 0.10 under wet lubrication. These previous studies suggest that the lubricating mechanism works on the dry contact interface between the CS-SKD11 disc and the AISI304 ball to sustain a low frictional state.
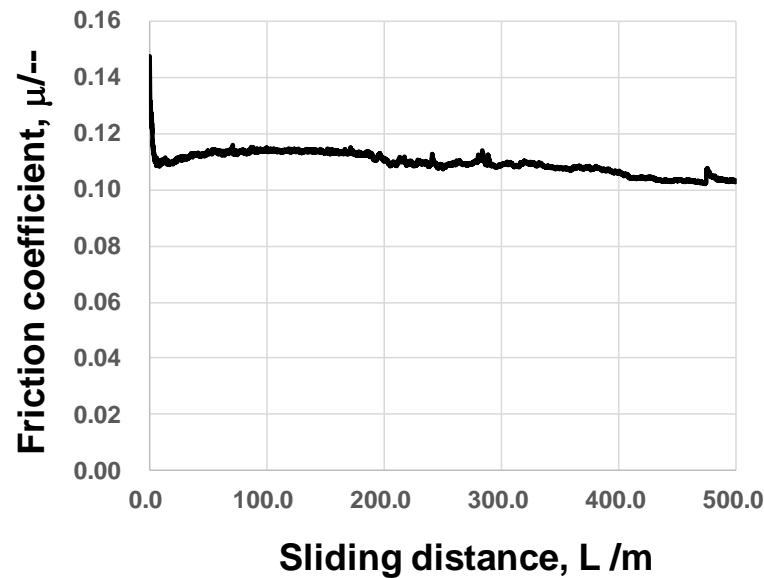
Figure 5. Variation in the frictional coefficient with changing the sliding distance in BOD testing.

SEM (scanning electron microscopy) and EDX (electron-dispersive X-ray spectroscopy) was utilized to investigate the interface on the wear track of the CS-SKD11 disc. Figure 6 shows the SEM image on the wear track and the element mapping of iron, chromium, nickel and carbon, respectively. Except for a trace of iron debris fragments, the whole wear track is covered by carbon in correspondence to the carbon peak detection in the energy spectrum via EDX. This proves that the free carbon solute diffuses from the carbon supersaturated tool steel disc to the contact interface and in situ forms a tribofilm to reduce the friction and adhesive wear. The normal stress gradient drives this unbound carbon diffusion through the carbon supersaturated tool steel grain boundaries to the contact interface.
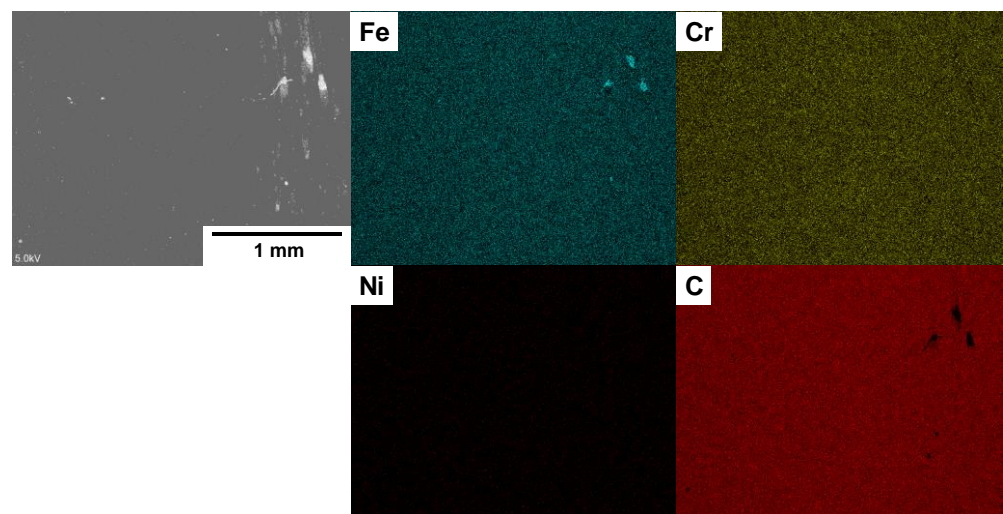
Figure 6. SEM image on the wear track and element mapping on the wear track after running the AISI304 ball in 500 m.

3.2. Fine Blanking Behavior of CS-YXR7 Punch with Square Head

The CS-matrix tool steel type YXR7 (CS-YXR7) punch was prepared for fine blanking the AISI304 austenitic stainless steel plate with a thickness of 2 mm. Its square punch head was sized 5.0 mm × 5.0 mm. Figure 7a depicts the AISI304 blank; as shown in Figure 7b, no fractured zones were detected on the sheared surface.
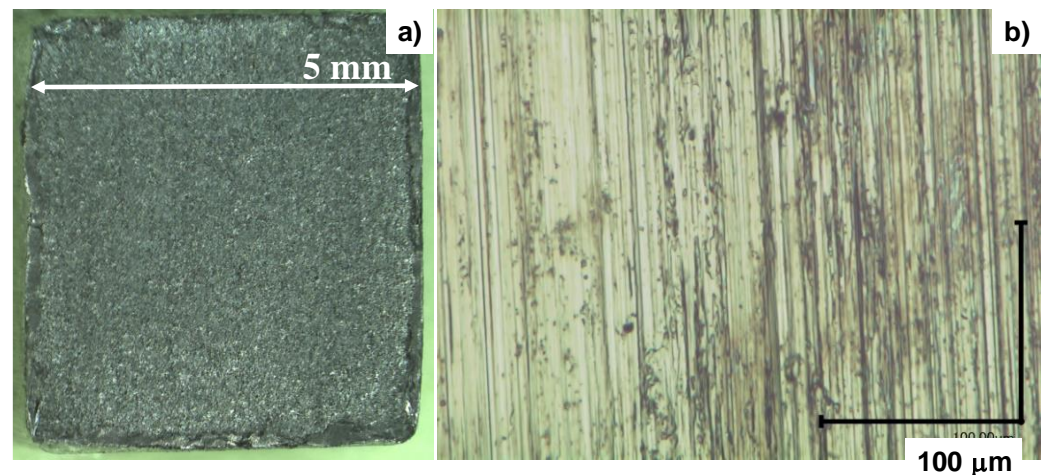
Figure 7. The sheared AISI304 blank using the CS-YXR7 punch with the square head. (**a**) Overview of sheared blank and (**b**) the sheared surface of blank.

Figure 8 shows the three-dimensional sheared surface profile of the AISI304 blank. No adhesive debris fragments were noticed, even locally. Under the clearance by 0.5% of AISI304 plate thickness, the fully burnished surface has a maximum roughness of 6.2 μm within the clearance of 10 μm. This well-sheared smooth surface reveals that the contact interface between the punch side surfaces and the AISI304 work is prevented from adhesive wear even under severe shearing during the fine blanking operation.
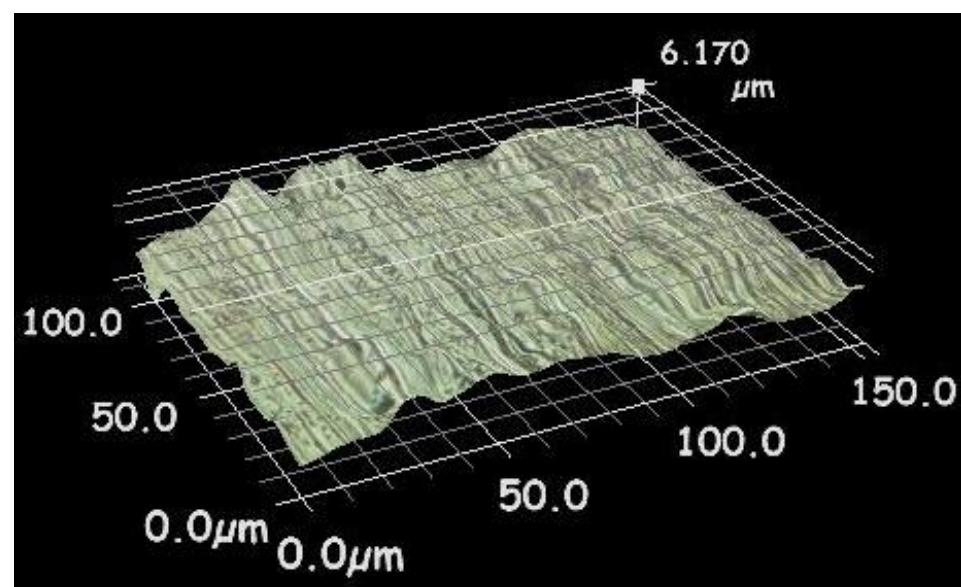

Figure 8. Three-dimensional profile of sheared surface.

3.3. Fine Blanking of Twelve-Tooth Gears with CS-YXR7 Punch

The CS-YXR7 punch with the twelve-tooth gear head was also prepared for fine blanking the AISI304 miniature gears. As depicted in Figure 9a, the punch head was designed and machined to have a twelve-tooth head. In this gear design with the module

1.0, the pitch circle diameter was 12.00 mm, the pressure angle was 20°, the top circle diameter was 14.00 mm, the root circle diameter was 10.00 mm, the tip radius was 0.3 mm, the root radius was 0.4 mm and no addendum was modified. After plasma carburizing as stated in 2.1, each punch edge profile was modified from a simple straight edge with a sharp corner to a skew-cut edge with an angled corner as designed in Figure 3b.
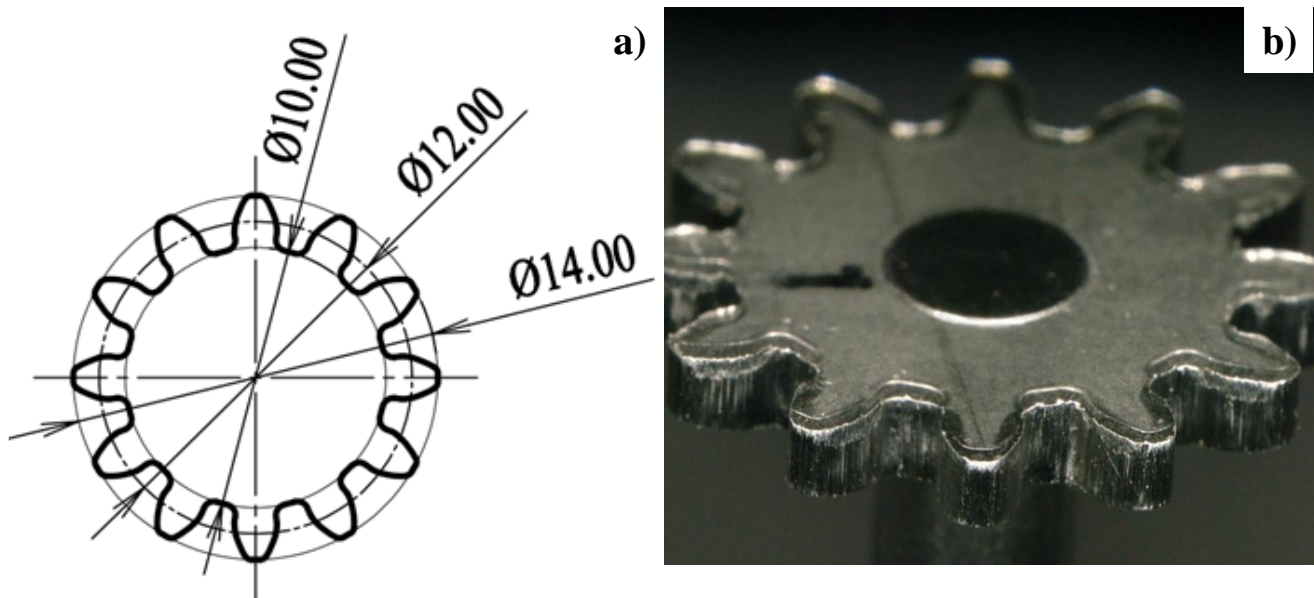
Figure 9. Comparison of the sheared AISI304 gear blank with the CAD data. (**a**) CAD geometric model and (**b**) sheared AISI304 gear blank at N = 50.

This shape-controlled CS-YXR7 punch was utilized for fine blanking the AISI304 plates to yield the AISI304 gears. The sheared AISI304 gear blank at N = 1 in Figure 9b is compared to the CAD model of module 1.0 gear in Figure 9a. Although burrs and troop are detected around the edges of the gear blank teeth, the circle diameters of the tooth top, tooth pitch and tooth root are reproduced to be 14.00, 12.00 and 10.00 mm, respectively, within a standard deviation of ± 0.02 mm. In the following, various dimensional deviations of gear blanks are measured to classify each item of dimensional accuracy into JIS (Japan Industry Standard) gear-grade.

3.4. Wear Resistance of CS-YXR7 Punch

In traditional fine blanking operations, punch edges often suffered from severe abrasive and adhesive wear with an increasing number of strokes (N). The punch edge indicated in Figure 3a was selected among twelve tooth edges. The variation of its punch edge profile was investigated at N = 1, 5, 10 and 50, respectively

As depicted in Figure 10, no worn-out zones and no adhesive fragments of AISI304 work are detected during the continuous fine blanking operations. In measurement, no significant changes were noticed in this anti-wearing behavior for other tooth edges in Figure 3a.

The contour measuring system was employed to measure the punch edge profile as indicated in Figure 3a. In correspondence to the finished edge profile in Figure 3b before experiment, the dimensional change of edge profile with N in the radial and longitudinal directions was measured offline at N = 0, 1, 2, 5, 10 and 50. Figure 11 compares the punch profiles at each stroke with the precise dimensional changes at the X–X section in the radial direction and at the Z–Z section in the longitudinal direction, respectively.
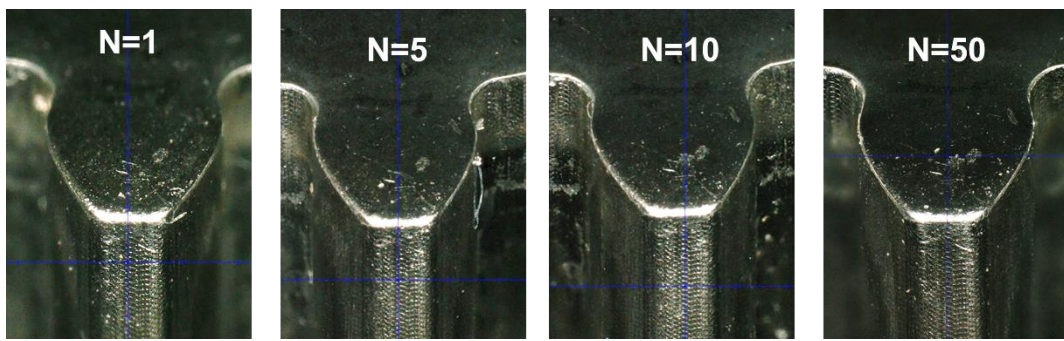
Figure 10. Punch edge profile change during the repeated fine blanking processes. The edge profiles were compared at N = 1, 5, 10 and 50.
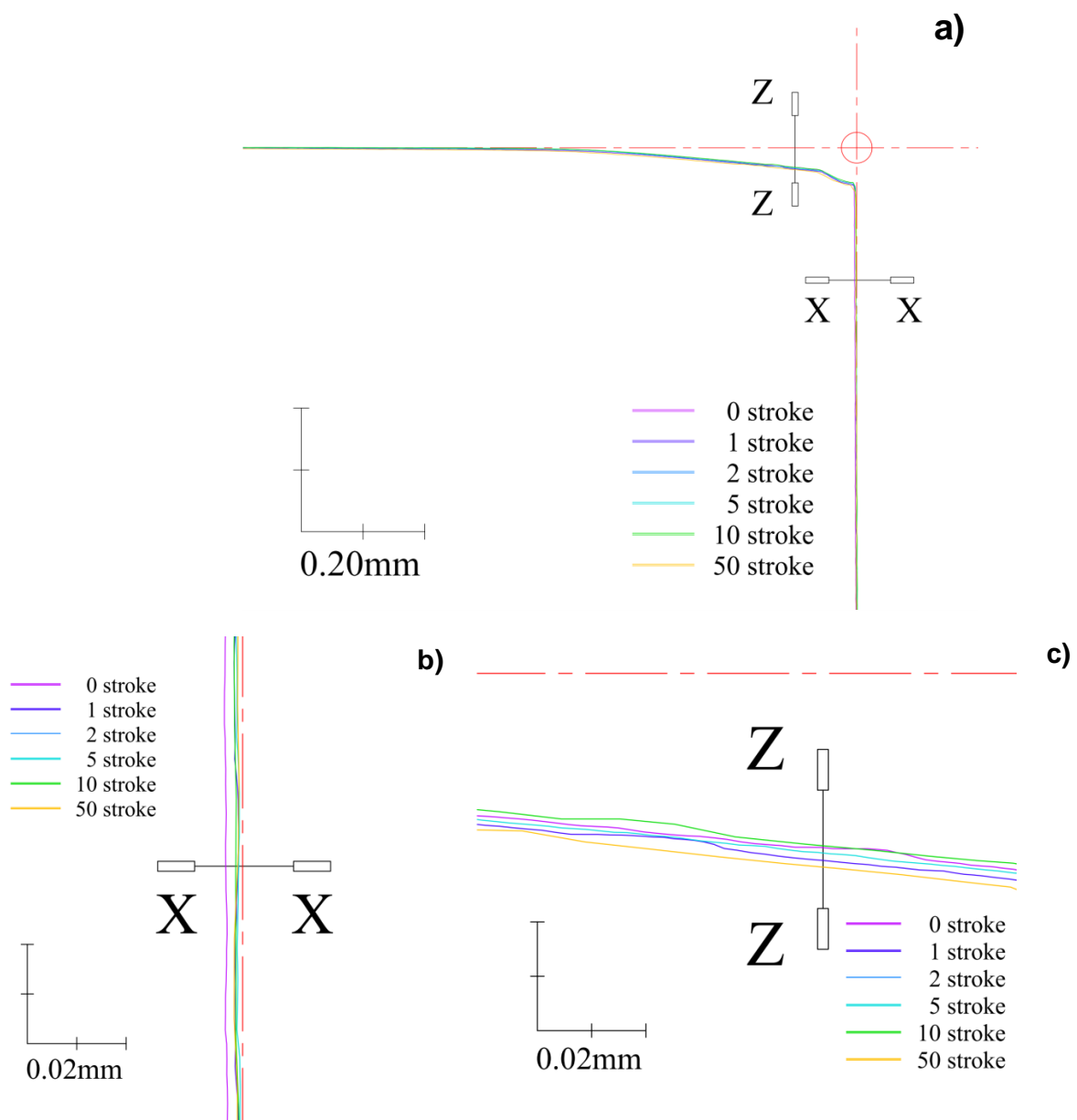

Figure 11. Precise measurement on the variation of edge profiles at N = 0, 1, 2, 5, 10 and 50. (**a**) Overview of the punch edge profiles at N = 0, 1, 2, 5, 10 and 50; (**b**) edge profile change at X–X with N; and (**c**) edge profile change at Z–Z with N.

The overall geometric configurations of punch edge profiles are compared in Figure 11a with increasing N. Even at 50, the punch edge profile is nearly the same as that before experiment. No significant abrasive and adhesive wear took place during the fine blanking process. This is in agreement with the offline contour measurement of punch edge profiles in Figure 10. In this punch edge profile, the precise dimensional changes at X–X and at Z–Z in Figure 11a were offline measured to describe the wearing behavior. As shown in Figure 11b, the punch width increased by +2.0 μm in the early stage from N = 0 to N = 10. This broadening of punch width was gradually suppressed after N = 10 and almost converged to +2.6 μm in maximum at N = 50. That is, little abrasive wear advances after the initial running-out till N < 50. On the other hand, the dimensional change at Z–Z in Figure 11c fluctuates within 3.6 μm at maximum. With consideration of the dimensional inaccuracy in fixing the punch in measurement, this fluctuation of edge profiles at N = 0, 1, 2, 5, 10 and 50 is smaller than the tolerance of measurement. No abrasive and adhesive wear took place at Z–Z in this continuous fine blanking operation.

3.5. Quality Evaluation on Blanked AISI304 Gears

The stable punch edge profile during fine blanking process reflects on the AISI304 gear-grade balancing. The pentagonal diagram on the fine-blanked gear-tooth dimensional deviations in Figure 4 is utilized to describe the gear-grade change with increasing the strokes.

As-blanked gears at N = 1 have heterogeneous dimensional deviations in the tooth geometries due to a little difference in the die setup and the clearance. Among five dimensional deviations, F_r and F_p are classified to JIS-5, but F_α and F_β are identified to be in the class of JIS-9 and JIS-10, respectively. These low grades in F_α and F_β might be caused by accumulation of dimensional distortions along the tooth alignment in gears. With increasing N, the dimensional inaccuracies in the punch and die shapes, the alignment inaccuracies in their positions at the die setup and the lubricating film thickness are all stabilized so that the gear-grade of blanks converges to be constant. In Figure 12, the irregular pentagonal diagram at N = 1, converges to a regular pentagon with nearly constant gear-grade from JIS-9 to JIS-10, at N = 50. This stabilization in the gear-grade balancing even without finishing process assures that as-blanked AISI304 gears are worth using as a mechanical element of industrial units.
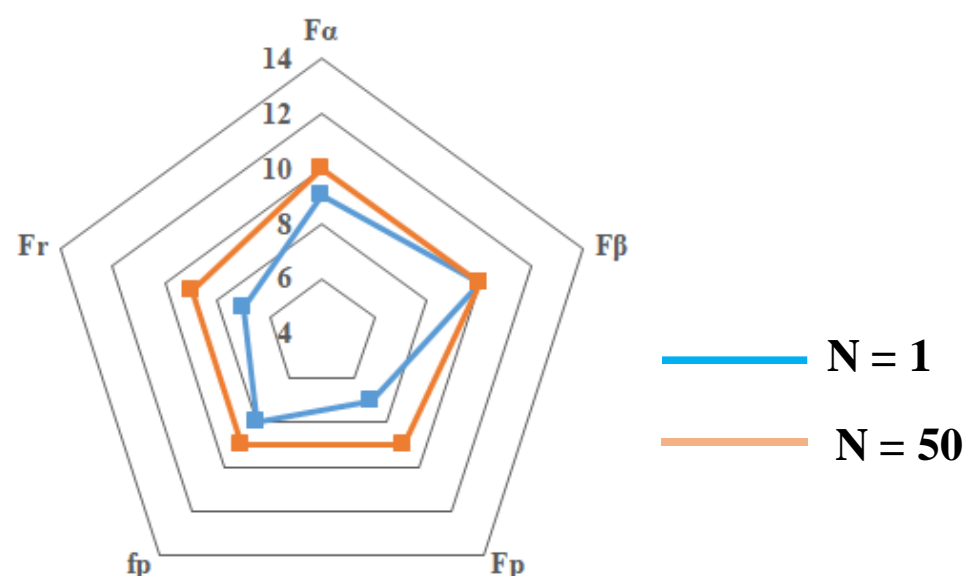
Figure 12. Gear-grade change with increasing the number of strokes on the gear-grade balancing diagram. The numbers inserted in the pentagonal diagram denote for the gear JIS-grade.

4. Discussion

Low friction and low adhesive wear are proven through the tribotesting of the CS-SKD11 disc against the AISI304 balls. During the sliding movement in rotation, the free-carbon tribofilm is in situ formed onto the highly stressed hot spots in the wear track to sustain the low frictional state with μ = 0.11 and to gradually reduce the friction coefficient down to μ = 0.10 with the running distance, L. The iron debris fragments deposit on the wear track in the trace levels. Most of wear track is free from adhesion of work materials. This low friction and adhesive wear behavior by the in situ formation of free carbon tribofilms just corresponds to the in situ solid lubrication mechanism during the fine blanking process, to be discussed later.

This low friction and wear state is also preserved in the fine blanking through using the CS-YXR7 punch with the square head. Fully burnished surface without adhesion of work debris fragments reveals that the shearing process becomes galling-free via the in situ formation of free carbon tribofilms. As stated in [11,12], the traditional fine blanking punches and dies without CS-treatment suffered from severe adhesion of work materials onto their surfaces when shearing the ductile works such as the austenitic stainless steels, the pure titanium and titanium alloys. Furthermore, those punch edges and edge corners were inevitably worn out through abrasive wearing to reduce the punch life. The edge profile control must be performed to improve the punch life within the dimensional tolerance of blanked products. When fine blanking the AISI304 gears, no essential difference is noticed between the punch edge profiles at N = 1 and 50. This proves that no abrasive wear occurs at the punch edges and edge corners to prolong the punch life in mass production of AISI304 gears in practice.

In the literature, a hard coating was thought as the first aid to reduce the adhesive and abrasive wears in metal forming. As had been reported in [19–21], the DLC (Diamond-Like Coating) and the nitride coating such as TiAlN, CrAlN, or TiAlSiN, work as a hard surface layer with engineering durability in various processes in metal forming. However, most of them suffered from a high friction coefficient due to adhesive wear when forming the titanium and austenitic stainless steels [22,23]. In addition, their coating thickness is too thin to be post-treated for edge profile control. Furthermore, their local delamination onsets the significant adhesion of work materials as reported in [24]. Hence, the coating procedure only provides a limited way to prevent the fine blanking punch from adhesive galling and abrasive wears.

Let us consider the role of in situ solid lubrication process in the present procedure. This in situ solid lubrication mechanism consist of three steps. At the first step, the carbon supersaturated layer is formed as a relatively thick carburized surface layer with the two-phase and nano-grained microstructure. This layer has high hardness of 1200 HV via the plasma carburizing at 673 K for 14.4 ks [8–10]. Through the STEM (Scanning transmission Electron Microscopy), this two-phase, nano-grained layer consist of the carbon-rich and carbon-poor nano-sized clusters. This implies that the supersaturated, unbound carbon solutes are present in the phase-separated nanoscopic clusters with high content. In the step-II, these excess unbound carbon solutes diffuse through the nanoscopic cluster boundaries from the depth to the surface under the stress gradient in shearing the AISI304 work materials. The diffusing free carbon solutes form a thin tribofilm on the highly stressed hot spots of contact interface to sheared work materials in the step-III. With increasing the strokes in fine blanking, the initially formed free-carbon tribofilm is stabilized on the contact interfaces between the CS-punch and AISI304 work. This sustainable presence of carbon tribofilm results in the gradual decrease in the friction coefficient in Figure 5 and in the low distortion of punch edge profiles in Figure 11.

In the present post-treatment, the punch edge profile was finished before plasma carburizing. In the similar manner to the post-treatment of thick DLC and diamond coatings, the plasma carburized layer has enough thickness to be post-treated for adjusting the punch edge profiles without deterioration to in situ solid lubrication mechanism in the

above. In fact, the edge profile of plasma nitrided SKD11 punches was post-treated to have sharpness enough to improve the punching behavior of electrical steel sheets [25].

The as-blanked AISI304 gears have dull troop and burrs so that the gear-grade balancing is deteriorated in general. In particular, the initial grade of blanked gears at N = 1 have heterogeneous JIS-grade balance as shown in Figure 12. This initial irregular pentagon of unbalanced gear-grades is improved to be a more regular and smaller pentagon through the optimization of carbon supersaturation process and through the carbon supersaturation of punch and die pair. In particular, the average carbon solute content and the hardness profile have much influence on the reduction of dimensional inaccuracies during the fine blanking operation.

As reported in [26], high stiffness of gears has become an essential keyword in reducers for robotics and electric vehicles. The austenitic stainless steel gears work as a high-strength and toughness element to drive the sliding and rotational movement as designed. The fine blanking provides a solution for mass production of stainless steel gears with high gear-grade. The sufficient CS-punch life is preserved for this mass production for N >> 50 since no adhesive and abrasive wears are detected on the twelve punch edge profiles even when increasing the strokes, as demonstrated in Figure 11. This possibility of engineering durability of CS-punch and die in long term usage becomes attractive to fine blanking and forging of stainless steel preforms. Much less adhesion of fresh work materials onto CS-dies prolongs a die life in continuous blanking and forging. As explained in [12,27], low friction and low work hardening during blanking and forging steps, reduces the energy consumption even in the multi-step fabrication of complex-shaped stainless steel parts.

5. Conclusions

Carbon supersaturation prevents adhesive wear to the fine blanking punch even under the severe shearing operation of austenitic stainless plates. With aid of punch edge profile control, it is also free from abrasive wear after continuous fine blanking strokes in long-term mass production. Little edge profile change from the initial state demonstrates that the CS-punch with a tailored edge profile works as a reliable tool for fine blanking in mass production. The AISI304 gear-grade balancing is improved to be within JIS-9 to JIS-10 grades after fine blanking operations in the early stage, even without finishing steps. This suggests that carbon-supersaturated punch and die with punch and die edge profile control is a superior procedure to the coated punch and die pair in the normal approach with only single-chamfered punch edge corners.

The CS-die with CS-punch improves the shearing behavior with less adhesive and abrasive wearing. The precise tuning in carbon supersaturation through the adjustment of plasma carburizing parameters provides a way to reduce dimensional distortion during fine blanking. The titanium and stainless steel gears with higher JIS gear-grades come true through the fine blanking process with the use of advanced special CS tools. With aid to the forging process from CS-dies, the preforged stainless steel preform was accurately fine-blanked using CS-dies to fabricate the spur and bevel gears with much less damage than the conventional forging processes and with comparable gear-grade balancing to normally cut gear-grades.

Informed Consent Statement: Informed consent was obtained from all subjects involved in the study.

Data Availability Statement: MDPI Research Data Policies at https://www.mdpi.com/ethics (accessed at 7 September 2023).

References

1. Law, I. *Gears and Gear Cutting for Home Mechanists*; Fox Chapel Publishing: Mount Joy, PA, USA, 2018.
2. Beddoes, J. *Introduction to Stainless Steels*, 3rd ed.; ASM: Materials Park, OH, USA, 1999.
3. MacMaster. Available online: https://www.mcmaster.com/stainless-steel-gears/ (accessed on 9 February 2023).
4. Southern Gears. Available online: https://southerngear.com/stainless-steel-gears/ (accessed on 9 February 2023).
5. Feuerhack, A.; Trauth, D.; Mattfeld, P.; Klocke, F. *Fine Blanking of Helical Gears. 60 Excellent Inventions in Metal Forming*; Elsevier: Amsterdam, The Netherlands, 2015; pp. 187–192.
6. Moghadam, M.; Villa, M.; Moreau, P.; Dubois, A.; Dubar, L.; Nielsen, C.V.; Bay, N. Analysis of lubricant performance in punching and blanking. *Tribol. Int.* **2020**, *141*, 105949. [CrossRef]
7. Zheng, Q.; Zhuang, X.; Gao, Z.; Guan, M.; Ding, Z.; Hong, Y.; Zhao, Z. Investigation on wear-induced edge passivation of fine-blanking punch. *Int. J. Adv. Manuf. Technol.* **2019**, *104*, 4129–4141. [CrossRef]
8. Li, X.; Du, N.; Feng, C.; Chen, K.; Wei, X.; Zhang, D.; Lee, K.-R. Theoretical superlubricity and its friction stability of amorphous carbon film induced by simple surface graphitization. *Appl. Surf. Sci.* **2023**, *615*, 156318. [CrossRef]
9. Ge, X.; Chai, Z.; Shi, Q.; Liu, Y.; Wang, W. Graphene superlubricity: A review. *Friction* **2023**, *11*, 1953–1973. [CrossRef]
10. Argibay, N.; Babuska, T.F.; Curry, J.F.; Dugger, M.T.; Lu, P.; Adams, D.P.; Nation, B.L.; Doyle, B.L.; Pham, M.; Pimentel, A.; et al. In-situ tribochemical formation of self-lubricating diamond-like carbon films. *Carbon* **2018**, *138*, 61–68. [CrossRef]
11. Aizawa, T.; Fuchiwaki, K. Galling-free fine blanking of titanium plates using carbon-supersaturated high-speed steel punch. *C* **2023**, *9*, 15. [CrossRef]
12. Li, Y.; Zhao, Y.; Hao, Y. Numerical simulation of fine blanking die wear and die performance analysis. *J. Chem.* **2022**, *2022*, 9893356. [CrossRef]
13. Aizawa, T.; Fuchiwaki, K.; Dohda, K. Galling-free fine blanking of titanium plates by carbon supersaturated tool steel punch. *Mater. Res. Proc.* **2023**, *28*, 869–878.
14. Suzuki, Y.; Shiratori, T.; Murakawa, M.; Yang, M. Precision stamping process of metal micro gears. *Procedia Manuf.* **2018**, *15*, 1445–1451. [CrossRef]
15. Aizawa, T.; Yoshino, T.; Suzuki, Y.; Shiratori, T. Free-forging of pure titanium with high reduction of thickness by plasma carburized SKD11 dies. *J. Mater.* **2023**, *14*, 2536. [CrossRef] [PubMed]
16. *JIS B 1702-1 2016*; Gear Grade Balancing. JSA (Japan Standard Association): Tokyo, Japan, 2019.
17. Wang, W.; Hua, M.; Wei, X. Friction behavior of SUS304 metastable austenitic stainless sheet against DC53 die under the condition of friction coupling plastic deformation. *Wear* **2011**, *271*, 1166–1173. [CrossRef]
18. Dib, J.; Herenu, S.; Ali, D.; Pellegri, N. Influence of load, surface finish and lubrication on friction coefficient of AISI304 stainless steel. *J. Mater. Eng. Perform.* **2020**, *29*, 2739–2747. [CrossRef]
19. Nunthavarawong, P.; Rangappa, S.M.; Siengchin, S.; Dohda, K. (Eds.) *Diamond-like Carbon*; Technologies and Applications; CRC-Press: Boca Raton, FL, USA, 2023.
20. Terek, P.; Kovacevic, L.; Miletic, A.; Skoric, B.; Kovac, J.; Drnovsek, A. Metallurgical soldering of duplex coating in contact with aluminum alloy. *Coatings* **2020**, *10*, 303. [CrossRef]
21. Fernandies, L.; Silva, F.J.G.; Alexandre, R. Study of TiAlN PVD coating on stamping dies used in tinplate food package production. *Micromachines* **2019**, *10*, 182. [CrossRef]
22. Dohda, K.; Aizawa, T. Tribo-characterization of silicon doped and nano-structured DLC coatings by metal forming simulators. *Manuf. Lett.* **2014**, *2*, 82–85. [CrossRef]
23. Ding, Q.; Wang, L.; Hu, L. Tribology optimization by laser surface texturing: From bulk materials to surface coatings. Ch. 16. In *Laser Surface Engineering*; Processes and Applications; Woodhead Publishing: Cambridge, UK, 2015; pp. 405–422.
24. Okitsu, Y.; Miyake, H.; Shinmiya, T.; Yamasaki, Y. Effects of PVD coating properties on die damage in piercing of 1470-MPa-class ultrahigh-strength steel sheet. *J. Stat. Theory Pract.* **2023**, *64*, 57–64. [CrossRef]
25. Aizawa, T.; Shiratori, T.; Yoshino, T.; Suzuki, Y.; Dohda, K. Quantitative characterization of the affected zones in a single crystal Fe-6Si steel sheet by fine piercing. *Micromachines* **2022**, *13*, 562. [CrossRef] [PubMed]
26. Ando, K. Future prospects and current situation of the robot reduction gear. *Robotics* **2015**, *33*, 329–333.
27. Ishiguro, S.; Aizawa, T.; Funazuka, T.; Shiratori, T. Green forging of titanium and titanium alloys by using the carbon supersaturated SKD11 dies. *J. Appl. Mech.* **2022**, *3*, 724–739. [CrossRef]